EPI International Journal of Engineering
Volume 8, Number 2, August 2025, pp. 122-127
DOI: 10.25042/epi-ije.082025.09

*p*ISSN 2615-5109
*e*ISSN 2621-0541

Slope Stability Analysis at JLS Lot 3 Blitar with Soil Nailing Reinforcement under Seismic Loading using Finite Element Method

Siti Fauziah[a,*], Yerry Kahaditu Firmansyah[b], Bagas Aryaseta[c], Miguel Felix Wijaya[d]

[a]Department of Civil Engineering, Faculty of Engineering and Science, Universitas Pembangunan Nasional "Veteran" Jawa Timur. Email: 22035010040@student.upnjatim.ac.id.
[b]Department of Civil Engineering, Faculty of Engineering and Science, Universitas Pembangunan Nasional "Veteran" Jawa Timur. Email: yerry.kahaditu.ts@upnjatim.ac.id.
[c]Department of Civil Engineering, Faculty of Engineering and Science, Universitas Pembangunan Nasional "Veteran" Jawa Timur. Email: bagas.aryaseta.ts@upnjatim.ac.id.
[d]Department of Civil Engineering, Faculty of Engineering and Science, Universitas Pembangunan Nasional "Veteran" Jawa Timur. Email: miguel_felix.ts@upnjatim.ac.id.

Abstract

Slope stability in hilly areas with high seismic activity requires thorough geotechnical assessment to prevent potential failures that could endanger infrastructure and human safety. This study evaluates the effectiveness of soil nailing combined with shotcrete in reinforcing slopes under both static and seismic conditions at JLS Lot 3, Blitar. A two-dimensional finite element method (FEM) with plane strain modeling was applied to simulate slope behavior, including staged construction procedures and soil-structure interaction. Soil parameters were derived from bore log data, corrected for groundwater table and overburden effects, and used to define unit weight, cohesion, internal friction angle, modulus of elasticity, and Poisson's ratio. The slope geometry was carefully modeled with attention to benching, slope angles, and shotcrete coverage. Surface loads representing construction, traffic, and pavement conditions were applied to the model to reflect realistic field scenarios. Results show that, without seismic loading, the reinforced slope reached a safety factor of 1.575, exceeding the minimum criterion of 1.50. When seismic loading was applied, the safety factor decreased to 1.106 but remained above the required 1.10 threshold, demonstrating that soil nailing with shotcrete effectively improves slope stability and controls deformation. The study emphasizes the importance of reinforcement design parameters, such as nail length, spacing, inclination angle, and shotcrete thickness, providing insights for optimizing slope reinforcement strategies under seismic conditions. The findings contribute to safer and more resilient slope design practices in earthquake-prone areas.

Keywords: FEM; seismic loading; shotcrete; slope stability; soil nailing

1. Introduction

The construction of road infrastructure in hilly areas within high seismic activity zones requires meticulous attention to geotechnical aspects, particularly slope stability. The southern coast of Java is a highly active tectonic zone due to the interaction between the Indo-Australian and Eurasian plates, which poses a significant risk of earthquakes and subsequent landslides. Such seismic events increase the inertial forces within the soil mass and reduce the soil's shear strength, thereby compromising slope stability [1]. Seismic loads are known to significantly decrease the Safety Factor (SF) of a slope, increasing the potential for deformation and failure [2]. This condition becomes more complex in heterogeneous and unsaturated soils, as the dynamic response of the soil is more sensitive to changes in stress and strain [3].

*Corresponding author. Tel.: +62-819-9125-2773
Universitas Pembangunan Nasional "Veteran" Jawa Timur
Surabaya, Indonesia, 60294

Figure 1. Landslide location at STA 1+075 – 1+100

In geotechnical engineering practice, a slope is considered stable if its Safety Factor meets the minimum criteria prescribed by SNI 8460:2017, which is SF ≥ 1.50 for static conditions and SF ≥ 1.10 under seismic loading. In the Southern Cross Road Project (Jalan Lintas Selatan - JLS) Lot 3, Serang Beach–Sumbersih, Blitar Regency, a landslide was recorded at STA 1+100. This incident was presumably triggered by cut-and-fill activities combined with high-intensity rainfall before the event. The alteration of slope geometry due to these construction works led to a redistribution of stresses within the soil mass, heightening the potential for instability, especially when subjected to seismic loads. The landslide condition at the study site is shown in Fig. 1.

Under these conditions, slope stability analysis requires an approach capable of representing soil behavior realistically. The Finite Element Method (FEM) is a numerical technique capable of modeling nonlinear stress-strain relationships of soil and providing a detailed distribution of deformations [4]. This method has been widely adopted in slope stability analysis due to its ability to yield results that are more representative of actual field conditions [5]. Furthermore, FEM allows for the modeling of slopes with complex geometries and diverse variations in soil parameters [6]. This method also provides more accurate deformation results compared to conventional methods [7].

Efforts to enhance slope stability through reinforcement methods continue to evolve, one of which involves the use of soil nailing. This technique works by increasing the internal shear resistance of the soil, thereby enabling it to withstand the deformations occurring within the slope [8]. It has been proven effective in significantly increasing the Safety Factor (SF) of slopes [9]. The effectiveness of soil nailing is influenced by design parameters such as nail length, inclination angle, and spacing between the soil nails. Consequently, a comprehensive analysis is required to optimally evaluate the performance of the reinforcement [10].

Despite extensive research on earthquake-induced slope stability and reinforcement methods, most studies treat these two aspects separately. Many finite element-based slope stability analyses also tend to focus solely on the final state, disregarding the construction sequence [11]. A more comprehensive numerical approach is required to analyze slope conditions under multifactorial influences [12]. Furthermore, FEM-based analysis enables a more detailed evaluation of soil-structure interaction [13] and provides a more realistic modeling of slope failure mechanisms [14].

Moreover, studies that integrate slope geometry alterations due to cut-and-fill operations, field-test-based soil parameters, and soil nailing performance evaluation within a single finite element framework remain highly limited. Based on these conditions, this study aims to analyze slope stability at JLS Lot 3, Blitar under seismic loading and evaluate the effectiveness of soil nailing reinforcement using FEM, with a focus on the final slope condition. This analysis is conducted to determine whether the planned reinforcement can increase the safety factor according to SNI 8460:2017 and to provide safe and efficient design recommendations.

2. Method

This study employs finite element analysis (plane strain) to evaluate slope stability under pseudostatic seismic loading. This approach was selected for its capability to accurately represent soil behavior and soil-structure interaction, ensuring results that closely align with actual field conditions.

2.1. N-SPT data and soil parameters

Soil data were obtained from bore log investigations conducted at the project site. Standard Penetration Test (N-SPT) values were taken from the boreholes nearest to the slope location and are summarized in Table 1.

The obtained N-SPT values were not used directly; they were corrected for the effects of groundwater table and overburden pressure, then correlated to derive soil parameters including unit weight (γ), cohesion (c), internal friction angle (φ), modulus of elasticity (E), and Poisson's ratio (ν), as presented in Table 2. The soil was modeled using the Mohr-Coulomb model, which can effectively represent the elastoplastic behavior of soil in a simple manner for slope stability analysis. The analysis was conducted assuming drained conditions, considering that the dominant soil type is sandy limestone.

Table 1. *N-SPT* data from Bore Log

Depth (m)	Soil Description	*N-SPT*
0 – 12.5	Slightly silty limestone	60.00
12.5 -13.5	Silty sandy limestone	60.00
13.5 - 15	Slightly silty limestone	60.00
15 – 15.5	Silty sandy limestone	60.00
15.5 - 28	Slightly silty limestone	60.00
28 – 29.5	Limestone with sandy clayey silt	60.00
29.5 - 31	Slightly silty limestone	60.00
31 – 36.5	Silty sandy limestone	59.33

Table 2. Soil parameters for finite element modeling

Layer	Type	γ_{unsat}	γ_{sat}	E	nu	c	φ
		kN/m^3	kN/m^3	MPa		kN/m^2	°
1	Drained	21.40	23.25	250	0.15	17.0	35.00
2	Drained	21.75	23.47	250	0.15	17.0	35.00
3	Drained	20.22	22.50	250	0.15	17.0	35.00
4	Drained	18.70	21.53	250	0.15	24.0	35.00
5	Drained	19.97	22.34	250	0.27	22.0	22.13
6	Drained	19.62	22.14	220	0.40	17.0	23.00
7	Drained	19.13	21.81	250	0.28	20.5	21.00
8	Drained	20.54	22.71	200	0.25	21.0	21.67

2.2. Slope geometry

Slope geometry was modeled based on existing field conditions derived from cross-sectional data. The modeling was performed under two-dimensional plane strain conditions. The soil stratification was modeled using bore log data with corrected and correlated parameters, then analyzed using a "fine" mesh setting. The slope modeling was conducted through staged construction simulations of each bench excavation to evaluate stability during construction before the final geometry was achieved. Table 3 details the geometric parameters used.

Table 3. Slope geometry parameters

Parameter	Symbol	Value	Unit
Total Slope Height	(*H*)	24	m
Number of Benches	(*h*)	6	-
Height per Bench	(*n*)	4	m
Width per Bench	(*b*)	2	m

2.3. Seismic loading

Seismic effects were modeled using a pseudostatic approach by incorporating the horizontal seismic coefficient (kh). The Peak Ground Acceleration (PGA) was determined to be 0.46 g, obtained from the 2021 Indonesia Design Spectra, based on the specific coordinates of Blitar City, aligning with the study site. Fig. 2 shows the design response spectrum for Blitar City, while Table 4 summarizes the corresponding input parameters used for the spectrum.

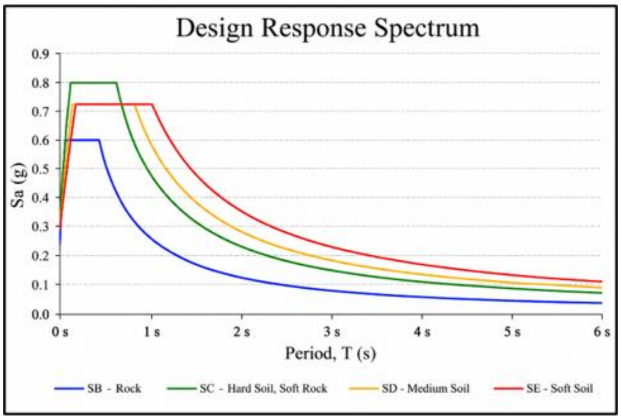

Figure 2. Design response spectrum for Blitar city

Table 4. Design spectrum parameters for Blitar City

Parameter	Value	Unit / Description
PGA MCEG	0.4600	(g) bedrock
SS MCEr	1.0015	(g) bedrock
S1 MCEr	0.4585	(g) bedrock
TL	20	seconds

The site amplification factor (F_{PGA}) was obtained through interpolation of the site coefficient tables relative to the site classification. Based on the average Standard Penetration Test (SPT) values from the bore logs, which exceeded 50 ($\overline{N}_{SPT}$) > 50, the site is classified as Site Class SC (Hard Soil). Table 5 summarizes the calculation of the average *N-SPT* for each layer, while Table 6 presents the site amplification factor for *PGA* (F_{PGA}) by site class.

Table 5. Summary the calculation of average ($\overline{N}_{SPT}$)

Depth (m)		N-SPT	Layer Thickness (m)	d_i / N_i
i	*j*			
0	2	60	2	0.033
2	4	60	2	0.033
4	6	60	2	0.033
6	8	60	2	0.033
8	10	60	2	0.033
10	12	60	2	0.033
12	14	60	2	0.033
14	16	60	2	0.033
16	18	60	2	0.033
18	20	60	2	0.033
20	22	60	2	0.033
22	24	60	2	0.033
24	26	60	2	0.033
26	28	60	2	0.033
28	30	60	2	0.033
30	32	60	2	0.033
32	34	58	2	0.034
34	36	60	2	0.033
Sum			36	0.601
Average *N-SPT*			59.885	
Site Class			SC (Hard Soil)	

Table 6. Site amplification factor for *PGA* (F_{PGA})

Site Class	*PGA* ≤ 0.1	*PGA* = 0.2	*PGA* = 0.3	*PGA* = 0.4	*PGA* = 0.5	*PGA* ≥ 0.5
SA	0.8	0.8	0.8	0.8	0.8	0.8
SB	0.9	0.9	0.9	0.9	0.9	0.9
SC	1.3	1.2	1.2	1.2	1.2	1.2
SD	1.6	1.4	1.3	1.2	1.1	1.1
SE	2.4	1.9	1.6	1.4	1.2	1.1
SF			SS			

For site class SC, the F_{PGA} value at *PGA* = 0.4 is 1.2, and at *PGA* = 0.5 is also 1.2. Given that the Peak Ground Acceleration (*PGA*) at the study location is 0.46 g, linear interpolation is performed using the following equation:

$$F_{PGA} = F_1 + \frac{(PGA - PGA_1)}{(PGA_2 - PGA_1)}(F_2 - F_1) \qquad (1)$$

with the following parameters:

$F_1 = 1.2$ at $PGA_1 = 0.4$
$F_2 = 1.2$ at $PGA_2 = 0.5$
$PGA = 0.46$ g

resulting in:

$$F_{PGA} = 1.2 + \frac{(0.46-0.4)}{(0.5-0.4)}(1.2-1.2)$$
$$F_{PGA} = 1.2$$

The horizontal seismic coefficient, kh, was subsequently calculated using the following equations:

$PGA_M = F_{PGA}$ x PGA
= 1.2 x 0.46 = 0.552 g
k_h = 0.5 x PGA_M
= 0.5 x 0.552 = 0.276 g

The resulting *kh* value of 0.276 g is utilized in the pseudostatic analysis to represent the earthquake-induced forces on the slope stability.

2.4. Slope reinforcement

Slope reinforcement using soil nailing and shotcrete was integrated into the finite element analysis. In this model, soil nails were represented as embedded beams, while shotcrete was modeled as plate elements. These components enhance soil shear strength and control slope deformation. Reinforcement parameters are detailed in Tables 7 and 8.

Table 7. Soil nailing parameters

Parameter	Symbol	Unit	Value
Material Type	-	-	elastic
Nail Length	*L1*	(m)	12
	L2	(m)	12
	L3	(m)	16
	L4	(m)	18
	L5	(m)	20
	L6	(m)	22
Spacing	$L_{spacing}$	(m)	1.5
Hole Diameter	*D*	(m)	0.032
Distance	*Sv*	(m)	1.5
	Sh	(m)	1
Angle	*i*	(°)	20
Cross-sectional Area	*As*	mm^2	819
Yield Strength	*Fy*	MPa	420
Young Modulus	*E*	kN/m^2	$2x10^8$
Unit Weight	*γ*	kN/m^3	78.5

Table 8. Shotcrete parameters

Parameter	Value	Unit
Thickness	0.20	m
EA (Axial Stiffness)	5.14×10^6	kN/m
EI (Flexural Rigidity)	17135	kNm^2/m
Poisson ratio	0.20	-
Unit Weight	4.8	kN/m
Compressive Strength (*Fc'*)	30	MPa

3. Results and Discussion

Slope stability analysis was performed under two main conditions: the reinforced slope without seismic loading and the reinforced slope under seismic loading. The evaluation of slope stability was conducted using the strength reduction method to obtain the final Safety Factor (SF). In this method, the soil shear strength parameters are gradually reduced until numerical failure is reached. The results are then used to assess the effectiveness of soil nailing and shotcrete in enhancing slope stability under both static and seismic conditions.

3.1. Reinforcement model configuration

In the reinforced model, the soil nails were modeled as embedded beam rows, while the shotcrete layer on the slope surface was modeled as a plate element. Slope cutting was applied as an initial measure to reduce the driving force of the soil mass. Subsequently, soil nailing and shotcrete were installed to increase resisting forces and control slope deformation.

The reinforcement was installed with an inclination angle of 20°, vertical spacing of 1.5 m, and horizontal spacing of 1.0 m. This configuration was designed to connect the active soil mass to the more stable zone behind the potential slip surface. The reinforced slope model is shown in Fig. 3.

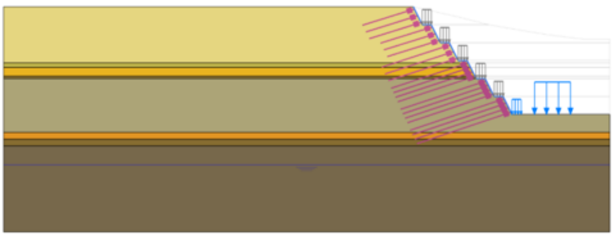

Figure 3. Reinforced slope model with soil nailing

3.2. Meshing and loading

Meshing was performed using a fine mesh density to improve modeling accuracy, particularly in the interaction zone between soil, soil nails, and shotcrete. A denser mesh was required to better represent the stress and deformation distribution around the reinforcement elements. The meshing output of the reinforced slope model is shown in Fig. 4.

In addition to the self-weight of the soil and reinforcement elements, the slope model also considered design loads applied to the slope surface. These loads consisted of construction load, traffic load, and pavement load. The details of the design loads are presented in Table 9.

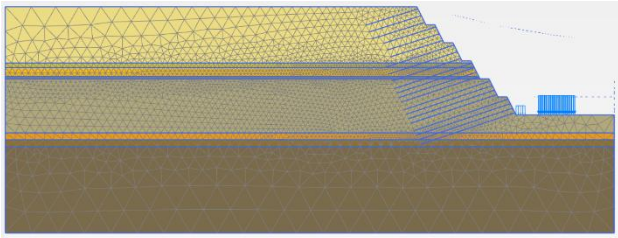

Figure 4. Mesh output of the soil-nailed slope model

Table 9. Design loads on slope surface

Traffic Load (*Load A*)	15	kN/m^2
Load of Pavement		
Asphalt Layer (AC - BC)	6	cm
Asphalt Layer (AC - WC)	4	cm
Base Course (Aggregate A)	20	cm
Unit Weight Asphalt	23	kN/m^3
Unit Weight Aggregate A	20	kN/m^3
Load of Asphalt	2.3	kN/m^2
Load of Aggregate A	4	kN/m^2
Total Load of Pavement (*Load B*)	6.3	kN/m^2
Total surcharge load (*Load A* + *Load B*)	21.3	kN/m^2

3.3. Reinforced slope analysis without seismic loading

The first analysis was conducted on the reinforced slope condition using soil nailing and shotcrete without seismic loading. Fig. 5 shows the reinforced slope model under this condition. The results indicate that the slope safety factor increased to 1.575, satisfying the minimum slope stability criterion for static conditions based on SNI 8460:2017 (SF ≥ 1.50). This demonstrates that the combination of slope cutting, soil nailing, and shotcrete effectively increases the resisting capacity of the slope and reduces the potential for failure. The detailed reached values from the FEM simulation are summarized in Table 10.

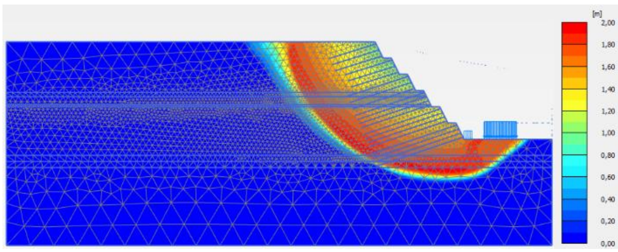

Figure 5. Reinforced slope model without seismic loading

Table 10. Safety factor of reinforced slope without seismic loading

Parameter	Reached Value	Unit
Reached total time	0.000	Day
CSP – Relative stiffness	1.309×10^{-4}	-
ForceX - Reached total force X	0.000	kN/m
ForceY - Reached total force Y	0.000	kN/m
Pmax - Reached max pp	0.000	kN/m^2
ΣM_{stage} - Reached phase proportion	0.000	-
ΣM_{weight} - Reached weight proportion	1.000	-
ΣM_{sf} - Reached safety factor	1.575	-

3.4. Reinforced slope analysis under seismic loading

The next analysis was performed by incorporating seismic loading using a pseudostatic approach. The horizontal seismic coefficient used in the analysis was kh = 0.276 g. Under this condition, the slope also received combined additional loads, including traffic load, construction load, and pavement load.

The analysis result shows that the safety factor of the reinforced slope under seismic loading is 1.106. This value still satisfies the minimum slope stability criterion under seismic loading based on SNI 8460:2017, namely SF ≥ 1.10. Although the SF decreased due to the additional earthquake-induced inertial force, the soil nailing system was still able to maintain slope stability. The deformation distribution, as illustrated in Fig. 6, also indicates that soil movement remained controlled by the reinforcement elements. The detailed results are summarized in Table 11, which presents the reached values from the FEM simulation.

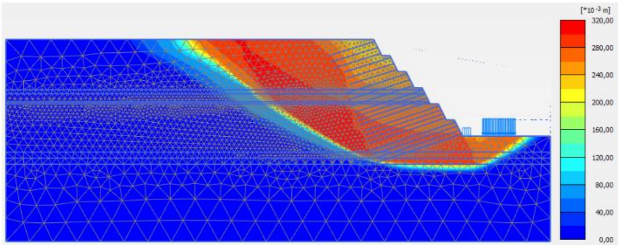

Figure 6. Reinforced slope model under seismic loading

Table 11. Safety factor of reinforced slope under seismic loading

Parameter	Reached Value	Unit
Reached total time	0.000	Day
CSP – Relative stiffness	1.678×10^{-4}	-
ForceX - Reached total force X	0.000	kN/m
ForceY - Reached total force Y	0.000	kN/m
Pmax - Reached max pp	0.000	kN/m^2
ΣM_{stage} - Reached phase proportion	0.000	-
ΣM_{weight} - Reached weight proportion	1.000	-
ΣM_{sf} - Reached safety factor	1.106	-

4. Conclusion

Several conclusions can be drawn from the slope stability analysis using soil nailing combined with shotcrete reinforcement. The analysis results indicate that the final safety factor (SF) of the reinforced slope under static conditions reaches 1.575, which satisfies the minimum requirement specified in SNI 8460:2017 (SF ≥ 1.50). This result demonstrates that the application of slope cutting combined with soil nailing and shotcrete effectively improves the resisting capacity of the slope. Under seismic loading conditions, the reinforced slope achieves a final SF value of 1.106, which also satisfies the minimum requirement of SNI 8460:2017 for seismic conditions (SF ≥ 1.10). Although the SF decreases due to the additional inertial forces generated during earthquakes, the reinforcement system remains capable of maintaining slope stability and limiting excessive deformation. Furthermore, based on the deformation distribution and obtained SF values, the combination of soil nailing and shotcrete can be considered effective in controlling soil movement and enhancing overall slope stability under both static and seismic conditions.

Based on these findings, several recommendations can be proposed for future studies and practical applications. Further evaluation of soil parameters through additional laboratory testing and field investigations is recommended to improve the accuracy and reliability of FEM modeling results. In addition, performing three-dimensional FEM analysis should be considered to better represent complex slope behavior and spatial variability of soil conditions. Future research may also incorporate dynamic seismic analysis, such as time-history analysis, to provide comparisons with the pseudostatic approach adopted in this study. Moreover, optimization of reinforcement parameters, including soil nail length, spacing, inclination angle, and shotcrete thickness, is recommended to obtain a more efficient and economical reinforcement design while maintaining the required level of slope stability.

References

[1] A. Ramayanti, F. Faris, and H. C. Hardiyatmo, "Effect of Parametric Soil Nailing under Seismic Behavior," *INERSIA Inf. dan Ekspose Has. Ris. Tek. Sipil dan Arsit.*, vol. 20, no. 2, pp. 164–174, 2024, doi: 10.21831/inersia.v20i2.74144.

[2] L. Teng, Y. He, Y. Wang, C. Sun, and J. Yan, "Numerical Stability Assessment of a Mining Slope using the Synthetic Rock Mass Modeling Approach and Strength Reduction Technique," *Front. Earth Sci.*, vol. 12, p. 1438277, 2024, doi: 10.3389/feart.2024.1438277.

[3] H. Basahel and H. Mitri, "Probabilistic Assessment of Rock Slopes Stability using the Response Surface Approach - A Case Study," *Int. J. Min. Sci. Technol.*, vol. 29, no. 3, pp. 357–370, 2019, doi: 10.1016/j.ijmst.2018.11.002.

[4] M. H. Mohamed, M. Ahmed, J. Mallick, and S. AlQadhi, "Finite Element Modeling of the Soil-Nailing Process in Nailed-Soil Slopes," *Appl. Sci.*, vol. 13, no. 4, p. 2139, 2023, doi: 10.3390/app13042139.

[5] A. A. Iftikhar and H. K. Artati, "Finite Element Modelling of Soil Nailing Inclination Effect on Slope Stability: Cibeureum Slope Case Study," *Teknisia*, vol. 29, no. 1, pp. 14–23, 2024, doi: 10.20885/teknisia.vol29.iss1.art2.

[6] S. Kazi and G. Rajpara, "Computational Modelling and Finite Element Analysis for Slope Stability Validation," *J. Inf. Syst. Eng. Manag.*, vol. 10, no. 3, pp. 1748–1763, 2025.

[7] N. Sabina and C. A. Makarim, "Proses Analisa Dinding Galian Basement 7 Lantai dengan Metode Elemen Hingga," *JMTS J. Mitra Tek. Sipil*, vol. 3, no. 1, p. 49, 2020, doi: 10.24912/jmts.v3i1.6980.

[8] A. R. Balu, I. M. Patuti, and F. Achmad, "Analisis Besaran Erosi dan Stabilitas Lereng dengan Perkuatan Soil Nailing," *J. Tek.*, vol. 23, no. 1, pp. 76–90, 2025, doi: 10.37031/jt.v23i1.614.

[9] D. P. Solin, A. Sefrina, and H. Farichah, "Pengaruh Soil Nailing terhadap Stabilitas Lereng menggunakan Software LEM dan Perhitungan Manual," *J. Konstr.*, vol. 16, no. 2, pp. 97–106, 2025, doi: 10.24853/jk.16.2.97-106.

[10] Y. W. PP and D. Setyanto, "Perhitungan Daya Dukung Pondasi Tiang Pancang Tunggal berdasarkan Data N-SPT dan CPT Studi Kasus: Proyek Pembangunan Stasiun Kereta Cepat Jakarta-Bandung," *J. Prakt. Keinsinyuran*, vol. 1, no. 2, pp. 81–94, 2024, doi: 10.25170/jpk.v1i02.6133.

[11] S. Suhaimah, Y. K. Firmansyah, and H. Farichah, "Analisis Penyebab Kelongsoran Lereng JLS LOT 3 menggunakan Metode Elemen Hingga," *Media Konstr.*, vol. 10, no. 2, pp. 175–185, 2025, doi: 10.33772/jmk.v10i2.129.

[12] K. Chand and R. Koner, "Large Dump Critical Zone of Interest Identification and Slope Failure Prediction using Realistic 3D Numerical Modelling," *Geomatics, Nat. Hazards Risk*, vol. 15, no.

1, 2024, doi: 10.1080/19475705.2024.2361809.

[13] J. W. Sihotang, T. Bakhtiar, N. Khoirullah, R. I. Sophian, and Z. Zakaria, "Slope Stability Analysis using Finite Element Method (FEM) in Wara Open Pit Coal Mine, PT Adaro Indonesia, Tabalong, South Kalimantan," *J. Geol. Sci. Appl. Geol.*, vol. 3, no. 3, pp. 13–18, 2019, doi: 10.24198/gsag.v3i3.25667.

[14] A. P. Putra and D. Syafriyandi, "Analisis Stabilitas Lereng dengan Metode Finite Element Method untuk Pembangunan Jembatan Wai Apu," *J. Eng.*, vol. 7, no. 1, pp. 1–10, 2025.